The complex cross-spectra of Cygnus X-2 and GX 5-1

van der Klis, M.; Hasinger, G.; Stella, L.; Langmeier, A.; van Paradijs, J.; Lewin, W.H.G.

Publication date
1987

Published in
Astrophysical Journal Letters

THE ASTROPHYSICAL JOURNAL, 319:L13–L18, 1987 August 1

THE COMPLEX CROSS-SPECTRA OF CYGNUS X-2 AND GX 5-1

M. VAN DER KLIS,[1] G. HASINGER,[2] L. STELLA,[1,3] A. LANGMEIER,[2] J. VAN PARADIJS,[4]
AND W. H. G. LEWIN[5]
Received 1987 April 2; accepted 1987 May 15

ABSTRACT

The intensity variations of Cyg X-2 and GX 5-1 are analyzed with a Fourier cross-spectral technique allowing to measure the frequency dependence of the time lags between the intensity variations in two X-ray spectral bands. In the 20–40 Hz frequency range of the quasi-periodic oscillations (QPO), the hard (~ 5–18 keV) signal lags the soft (~ 1–5 keV) one, while the reverse is true for the associated red noise. The observed time lags range from 0.4 to 8 ms. For similar QPO parameters, the observed lags are much smaller in GX 5-1 than they are in Cyg X-2. The "hard lags" previously measured in the cross-correlation functions of these sources are now identified as due to lags in the QPO. We argue that the "soft lags" now detected in the red noise are not inconsistent with the interpretation of the hard lags as due to inverse Compton scattering.

Subject headings: stars: individual (Cyg X-2, GX 5-1) — stars: pulsation — X-rays: binaries

I. INTRODUCTION

Intensity-dependent quasi-periodic oscillations (QPO) with frequencies in the 5–50 Hz range and, in some cases, red noise extending out to similar frequencies have been found with *EXOSAT* in the X-ray intensity of GX 5-1 (van der Klis *et al.* 1985), Cyg X-2 (Hasinger *et al.* 1986), and several other bright low-mass X-ray binaries (see van der Klis 1986*a* for a review).

GX 5-1 and Cyg X-2 both show similar bimodal X-ray spectral behavior, characterized by two branches in an X-ray hardness ratio versus intensity diagram. The properties of red noise and QPO, likewise bimodal, appear to be strictly correlated with spectral state (van der Klis *et al.* 1987*a*; Hasinger *et al.* 1987). In their so-called horizontal-branch (HB) spectral state, both sources show 18–45 Hz QPO, and red noise extending out to several tens of Hz. The QPO frequency shows a strong positive correlation with source intensity, the QPO have a hard X-ray spectrum (van der Klis 1986*a*; Hasinger 1986), and both QPO and red noise have relative amplitudes of a few percent. In the "normal branch" (NB) spectral state, no red noise above 1 Hz or QPO above 10 Hz are detected. In this state, Cyg X-2, at times, shows intervals of QPO with a frequency of ~ 5.6 Hz, which have a soft X-ray spectrum (Norris and Wood 1987; Hasinger 1986). In GX 5-1 there is an indication for ~ 5 Hz QPO in the NB state (van der Klis *et al.* 1987*a*).

In GX 5-1, rather steep red noise below 1 Hz is always present. It can be identified with the well-known variability of bright galactic bulge sources on all time scales down to 1 s and is likely related to variations in accretion rate. Flatter red noise extending out to ~ 20 Hz is only seen in the HB state (van der Klis *et al.* 1987*a*) and is apparently related to the 20–40 Hz QPO seen in this state. A very similar situation applies in Cyg X-2 (Hasinger *et al.* 1987). In accordance with previous usage, we shall designate the red noise component that only occurs in the HB state as LFN ("low-frequency noise") and the component that is always present below 1 Hz as VLFN ("very low frequency noise").

Hasinger (1986) recently calculated the cross-correlation function (CCF) between the intensity variations in two X-ray spectral bands for Cyg X-2 in the HB state. Functional fits to the CCF show that the "hard" (4.5–18.5 keV) variations lag the "soft" (0.7–4.5 keV) ones by several milliseconds. The lag, which was interpreted as the effect of inverse Compton scattering of the X-rays, decreases when the QPO frequency increases. This CCF-based analysis did not permit explicit determination of the frequency of the intensity variations contributing to the observed time lag. In this *Letter*, we study part of the same data on Cyg X-2 as used by Hasinger (1986), and in addition data on GX 5-1, with a Fourier cross-spectral technique which allows the frequency dependence of the time lags to be measured. A preliminary report of the cross-spectral analysis of the GX 5-1 data was given in van der Klis (1986*b*).

II. ANALYSIS AND RESULTS

All observations were performed using seven of the eight ~ 200 cm^2 argon-filled detectors of the *EXOSAT* Medium Energy instrument (Turner, Smith, and Zimmerman 1981). Simultaneous intensity measurements were made in four different photon energy channels with a time resolution of about 4 ms (1/256 s). Cyg X-2 was observed in its HB state for 12.5 hr on 1985 October 28–29, and in its NB state for 12.5 hr on 1985 November 15. GX 5-1 was observed in its NB state for

[1] *EXOSAT Observatory*, Astrophysics Division, Space Science Department of ESA.
[2] Max-Planck-Institut für extraterrestrische Physik.
[3] On leave from I.C.R.A., Department of Physics "G. Marconi," University of Rome.
[4] Astronomical Institute "Anton Pannekoek," University of Amsterdam.
[5] Massachusetts Institute of Technology, Center for Space Research and Department of Physics.

22 hr on 1985 August 27–28, and in its HB state for 12.5 hr on 1985 September 17. The energy channel boundaries were 0.7, 2.9, 4.5, 6.1, and 18.5 keV for Cyg X-2, and 1.2, 3.4, 5.8, 7.0, and 16 keV for GX 5-1.

Clear 18–45 Hz QPO were observed throughout both HB state observations; in the NB state observation of Cyg X-2, ~ 5.6 Hz QPO were clearly seen during a ~ 4 hr subset of the observations. The raw source intensities were 1000–1400 counts s^{-1} for Cyg X-2 and 1800–2200 counts s^{-1} for GX 5-1.

We divided the data into 32 s intervals of 8192 time bins each. The complex Fourier transforms of each 32 s interval were computed with an FFT technique separately for the summed intensities from the two lowest, and the two highest energy channels. The complex cross-spectrum of each interval was calculated by multiplying the complex Fourier amplitudes in the high-energy spectrum with the complex conjugates of those in the low-energy spectrum. The resulting complex cross-spectra were then summed together.

Due to dead-time–induced channel cross-talk, all complex Fourier amplitudes had large negative real parts. We corrected for this by subtracting the average complex Fourier amplitude in the 72–128 Hz range from the entire summed spectrum. This procedure is justified by the fact that in this frequency range the spectra are exclusively determined by Poisson noise, which at the 4 ms time resolution we used is by far the dominant source of variance, and therefore of channel cross-talk, at *all* frequencies. As no time lags naturally occur in the Poisson noise, which is confirmed by the fact that the average 72–128 Hz Fourier amplitude has no significant imaginary part, the procedure has no influence on the imaginary parts of the Fourier amplitudes of QPO and red noise, and hence on the sign of the time lags derived. In principle intensity-dependent dead-time effects can, in combination with temporally asymmetric flaring, cause apparent time lags. For the relatively low amplitudes of QPO and LFN in the present observations this effect is negligible.

For the NB state data, we also calculated the complex cross-spectra of 1024 s time intervals of 32,768 time bins each, making it possible to study the VLFN down to 0.001 Hz.

The resulting summed cross-spectra for the HB state observations are shown in Figure 1. The complex Fourier amplitudes are plotted as vectors (*short lines*), with their real parts along the positive Y-axis and their imaginary parts along the positive X-axis. For clarity, the points of origin of the vectors have been shifted along the frequency axis (*long diagonal line*). The figures are most easily interpreted as three-dimensional, with the frequency axis projecting out of the paper. With our choice of coordinates, vectors which are standing in an exactly vertical position on the frequency axis indicate *no* phase lag between the energy channels; vectors leaning to the left indicate a hard lag, vectors leaning right, a soft lag. The amount of phase lag is equal to the angle the vectors make with the positive Y-axis.

QPO and red noise are clearly seen in the cross-spectra of both sources. In the frequency range dominated by the red noise (below 10 Hz), most vectors lean to the right, indicating that the soft photons lag the hard ones. In the QPO range the opposite is the case. These effects are less pronounced in GX 5-1 than they are in Cyg X-2. Figure 2 shows the time lags implied by these complex cross-spectra as a function of frequency.

Average time lags for QPO and LFN were obtained by measuring the phase of the average vector in the 1–10 Hz range for the LFN, and in the range $\nu \pm \frac{1}{2}\lambda$ for the QPO. Here ν is the QPO frequency, and λ is the FWHM of the QPO peak as determined from a Lorentzian fit to the conventional power spectrum of the same data. The results are given in Table 1. Errors in the lags were determined by separately calculating the standard deviation in the scatter of the real and imaginary parts of the vectors in the individual 32 s

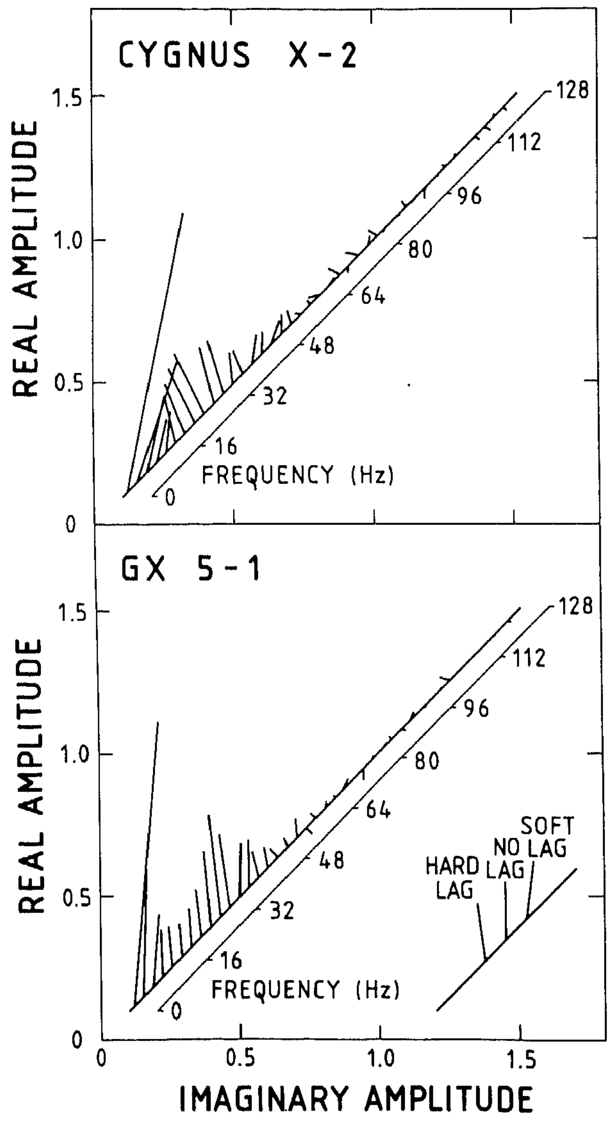

FIG. 1.—Time-averaged complex cross-spectra of the intensity variations in Cyg X-2 and GX 5-1 (see text). Long diagonal line is the frequency axis; short approximately vertical lines represent the complex vectors. Each vector is the average over a 3.125 Hz frequency interval. Vectors leaning left with respect to the vertical (Y-) axis indicate a hard time lag; vectors leaning to the right, a soft lag. Soft lags are observed in the red noise, while a hard lag is present in the QPO.

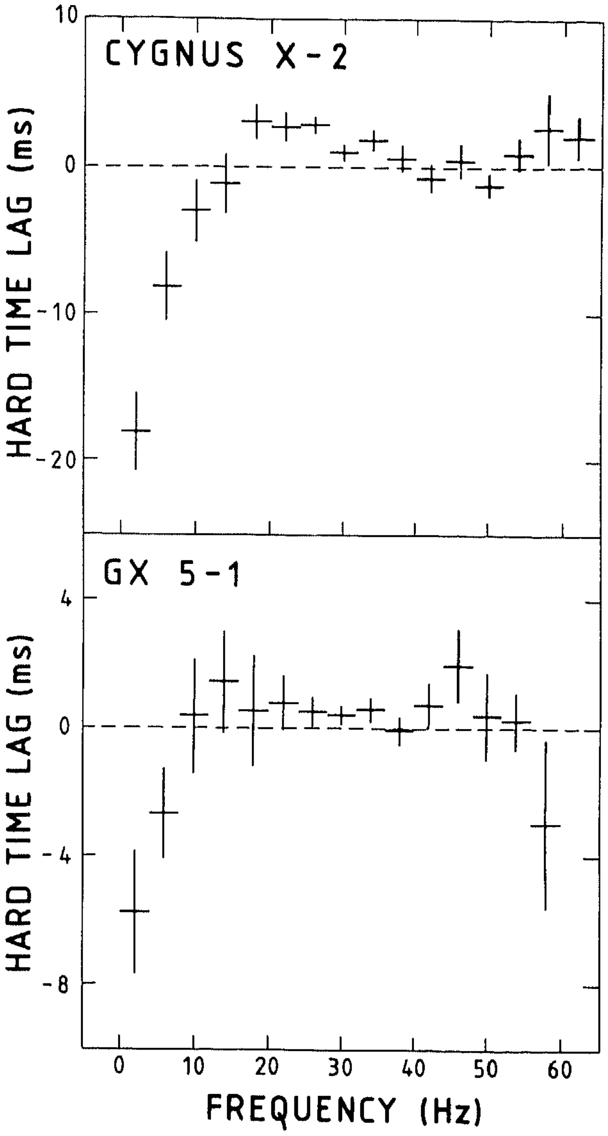

FIG. 2

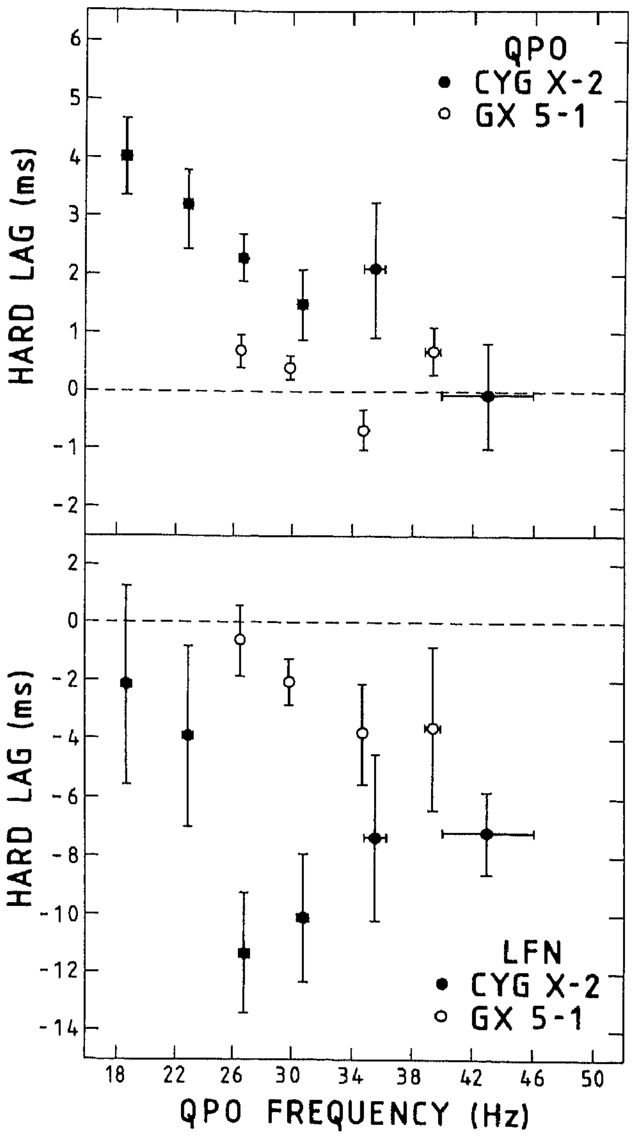

FIG. 3

FIG. 2.—Time lag spectra corresponding to the complex spectra in Fig. 1. Horizontal bars indicate frequency range; vertical bars represent 1 σ errors.

FIG. 3.—The dependence of the time lags on QPO frequency. LFN was measured between 1 and 10 Hz; QPO, in a frequency interval around the center of the peak with a width equal to the FWHM of the peak. Horizontal and vertical bars represent 1 σ errors.

TABLE 1

AVERAGE TIME LAGS IN HORIZONTAL BRANCH SPECTRAL STATE

		QPO		LFN	
SOURCE	ENERGY RANGES (keV)	ν-range (Hz)	Hard Lag (ms)	ν-range (Hz)	Hard Lag (ms)
Cyg X-2	0.7–4.5–18.5	20.5–34.2	2.2 ± 0.3	1–10	-7.9 ± 0.9
GX 5-1	1.2–5.8–16.0	21.2–38.3	0.44 ± 0.17	1–10	-2.3 ± 0.7

spectra and propagating these errors through the calculations. The errors thus include both the statistical uncertainties, and the scatter caused by the intrinsic variations in the QPO and LFN parameters. Phase lags were converted into time lags by dividing by the average frequency of the frequency range used in each case.

Note that for very similar average QPO parameters (frequency and FWHM) the lags observed in the HB state are different at a 5 σ level of confidence between the two sources for both QPO and LFN. This is not due to the different division between the hard and soft energy ranges (see Table 1): repeating the analysis for Cyg X-2 for the 0.7–6.1–18.5 keV ranges, we find very similar results (2.5 $\pm$ 0.4 and -8.0 ± 0.9 ms). The significance of the hard lag in the QPO in GX 5-1 is only 2.6 σ; however, from the analogy to Cyg X-2 we believe it is likely to be real.

As there exists a good correlation between source intensity and QPO frequency in our HB state observations, we were able to study the dependence of the time lags on QPO frequency by sorting the spectra according to intensity. The results are given in Figure 3. In Cyg X-2, there is a clear decrease in the hard time lag in the QPO as a function of QPO frequency. The time lags in the QPO of GX 5-1 do not show a clear trend, although they are formally incompatible with a constant value (98% confidence). The average lags derived previously from fitting the CCFs (Hasinger 1986; van der Klis 1986*b*) are very similar to (and can thus be identified with) the time lags derived here in the frequency range of the QPO; the soft lags in the LFN have practically no influence on the delays derived from the CCF fits. The reason for this is that the least-squares method used for these fits is much more sensitive to the steep variations in the CCF caused by the relatively high-frequency QPO than to the variations due to the LFN, which have a similar amplitude, but are much slower than those due to the QPO. The soft lags observed in the LFN are not found to be significantly variable as a function of QPO frequency.

Also when a possible dependence of the time lags on QPO frequency is considered, various statistical tests suggest that GX 5-1 shows significantly smaller lags in both QPO and LFN than Cyg X-2. For example, a linear fit to the hard lags in the QPO of Cyg X-2 gives $\chi^2 = 1.6$ for 4 d.o.f.; fitting to the data for both sources simultaneously gives $\chi^2 = 49$ for 8 d.o.f., rejecting the hypothesis that both data sets can be described with a single linear relationship.

In our NB state observations, there is, in some cases, a suggestion for a soft lag in the VLFN (below 1 Hz). However, any possible time lag in this frequency range should be treated with caution, as the large intensity fluctuations at these time scales imply considerable changes in the dead-time effects. The ~ 5.6 Hz QPO in Cyg X-2 (NB state) show a possible hard lag between the 0.7–2.9 keV and the 2.9–4.5 keV channels of 6.2 $\pm$ 2.7 ms (5.58–6.11 Hz).

III. DISCUSSION

a) *Soft Lags*

Many proposed QPO models allow a description of the signal underlying the power spectra in terms of oscillating shots. The shots themselves cause the LFN, while a quasi-periodic modulation of the shots is responsible for the QPO (see Lamb 1986). If inverse Compton scattering causes the oscillating shots in the hard band to lag those in the soft band

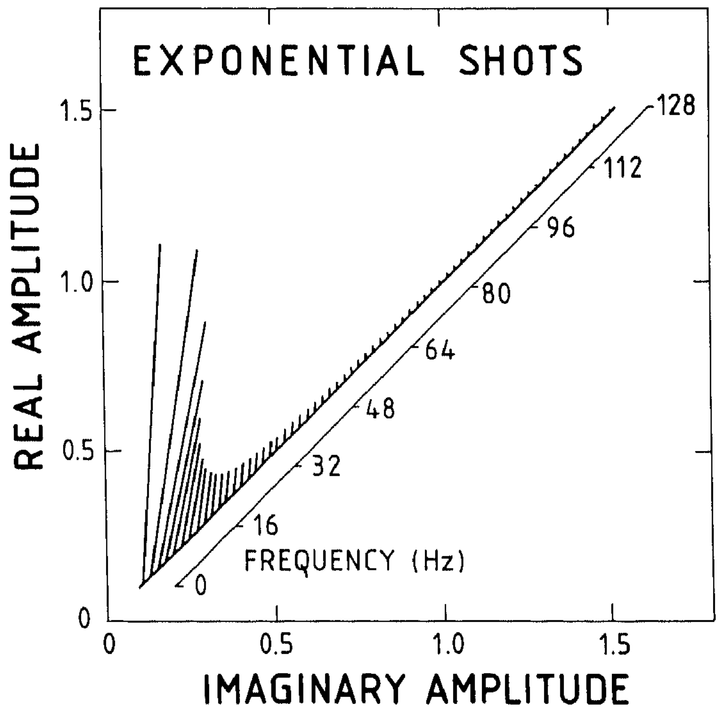

FIG. 4.—Simulated cross-spectrum of exponential shot noise. The shots have the same onset time in both bands. In the hard band the decay time is 20 ms; in the soft band, 30 ms. A "soft lag" in the red noise results.

without changing their time profile (because photons undergoing more inverse Compton scattering events will on average both get harder and take longer to emerge from the scattering medium), then QPO and LFN will undergo the same time shift. However, an apparent soft lag can occur in the LFN, if during the course of a shot the average X-ray spectrum softens and in that way shifts the temporal "center of gravity" of the soft shot with respect of that of the hard one. This apparent time shift (which will in general be somewhat frequency-dependent) can exceed that induced by Compton scattering. The soft lag observed in the LFN implies in this picture that the oscillating shots have a soft tail, a hard lead, or both. Figure 4 shows the result of a simulation of this effect using exponential shots with different decay times. So, the soft lag in the LFN revealed by our cross-spectral analysis does not invalidate the original interpretation (Hasinger 1986) of the hard lags in the QPO as caused by inverse Compton scattering. Whether the soft tail or the hard lead interpretation is the better one can in principle be determined from the relative duration of the shots in the two bands.

Softening of the shots is more easily accommodated by some QPO models than by others. In *self-luminous blob models* (e.g., Morfill and Trümper 1986) the oscillating shots are caused by short-lived blobs of matter spiraling in the inner disk. As the blobs spiral in, one would expect their temperature to rise and consequently their X-ray emission to get harder, contrary to our result.

In *reflection models* (e.g., Boyle, Fabian, and Guilbert 1986; Tennant 1987), the primary emission generated near the compact object is quasi-periodically reflected in our direction (by an oscillating accretion disk corona in the case of Boyle *et al.*, by blobs circulating in a disk in the case of Tennant). Unless the reflection process itself modifies the radiation (by Compton scattering), no softening of the shots would be expected. In the blob model of Tennant, again the blobs would be expected to get hotter and consequently the shots, if anything, harder.

In *accretion-modulation models* (e.g., Lamb *et al.* 1985) the accretion rate is itself modulated by oscillating shots. If shot noise in the accretion rate causes the emission of softening shots in the X-ray intensity, then one would expect to see soft lags from any similar accreting object (in these models a weakly magnetized neutron star) with a sufficiently variable accretion rate. It is not clear that this possibility can be excluded. The softening of the spectrum could be related to a gradually changing accretion rate during the shot. In the HB spectral state where we see the soft lags, the X-ray spectrum softens when the intensity increases. If this is also true on the time scale of the evolution of a shot, then the required spectral softening of the shots implies that the shots have a gradual rise and an abrupt decay. Alternatively, the softening shots could be the result of simple cooling of the just accreted plasma similar to the cooling of X-ray bursts after a thermonuclear flash.

In *obscuration models*, the QPO are explained by quasi-periodic partial obscuration of the X-ray emitting regions. The QPO–related LFN can be explained in such models by assuming that the emitting region that is being obscured shows a gradient in its X-ray surface brightness (van der Klis *et al.* 1987*b*). If this gradient is identified with a temperature gradient, then a softening of the average spectrum is a natural consequence of a decreasing oscillation amplitude of the obscuring medium (possibly a thick inner accretion disk): as the amplitude becomes smaller, the regions of highest temperature are progressively less exposed during an oscillation cycle. Hard Comptonization lags can in such a model arise in the same scattering medium that causes the QPO (see below).

b) *Hard Lags*

If the hard lags we observed in the QPO are caused by inverse Compton scattering, then the scattering process can not occur before the QPO are formed. Numerical simulations which will be presented elsewhere (Stollman *et al.* 1987) show that not only Comptonization of an oscillating signal by a stationary medium, but also Comptonization of a steady flux by a medium with oscillating scattering optical depth can cause QPO which show hard lags: the scattering can occur both after and during the formation of the QPO. The latter possibility might fit in with an obscuration scheme. The former one presents, as noted by Brainerd and Lamb (1987), problems for such a scheme.

In a Comptonization model the duration of the hard lags is determined by geometrical factors such as inclination, typical size R, and geometry of the scattering region, and by physical parameters such as Compton scattering optical depth τ, electron temperature T_e, and input photon spectrum. The average time Δt a photon spends in the scattering medium is only weakly dependent on T_e and roughly proportional to $R\tau$. The observed time lag δt between energy bands depends on the parameters in a more complicated way. For soft input spectrum and large τ, for example, δt is predicted to be *inversely* proportional to both τ and T_e (Pozdnyakov, Sobol, and Syunyaev 1983). Hence there are several possible explanations for the observed facts that the hard lag in Cyg X-2 becomes smaller when the QPO frequency increases, and that it is much larger than that in GX 5-1. The observed X-ray spectrum contains information about the physical parameters (τ, T_e, and incident spectrum), while the QPO frequency is in most QPO models determined by geometrical factors. Therefore, joint modeling of the lags, the QPO, and the X-ray spectrum is likely to provide more insight into the geometry and the physical circumstances in the inner emitting regions of the bright low-mass X-ray binaries.

W. H. G. L. acknowledges support from NASA (grant NAG8-571).

REFERENCES

Boyle, C. B., Fabian, A. C., and Guilbert, P. W. 1986, *Nature*, **319**, 648.
Brainerd, J., and Lamb, F. K. 1987, *Ap. J.* (*Letters*), **317**, L33.
Hasinger, G. 1986, in *IAU Symposium 125, The Origin and Evolution of Neutron Stars*, ed. D. J. Helfand and J. H. Huang (Dordrecht: Reidel), in press.
Hasinger, G., Langmeier, A., Sztajno, M., Pietsch, W., Gottwald, M., and Priedhorsky, W. 1987, in preparation.
Hasinger, G., Langmeier, A., Sztajno, M., Trümper, J., Lewin, W. H. G., and White, N. E. 1986, *Nature*, **319**, 469.

Lamb, F. K. 1986, in *The Evolution of Galactic X-Ray Binaries*, ed. J. Trümper, W. H. G. Lewin, and W. Brinkman (Dordrecht: Reidel), p. 151.
Lamb, F. K., Shibazaki, N., Alpar, M. A., and Shaham, J. 1985, *Nature*, **317**, 681.
Morfill, G. E., and Trümper, J. 1986, in *The Evolution of Galactic X-Ray Binaries* (Dordrecht: Reidel), p. 173.
Norris, J. P., and Wood, K. S. 1987, *Ap. J.*, **312**, 732.
Pozdnyakov, L. A., Sobol, I. M., and Syunyaev, R. A. 1983, *Soviet Sci. Rev. Section E: Ap. Space Phys. Rev.*, **2**, 189.
Stollman, G. M., Hasinger, G., Lewin, W. H. G., van der Klis, M., and van Paradijs, J. 1987, *M.N.R.A.S.*, in press.
Tennant, A. F. 1987, *M.N.R.A.S.*, in press.
Turner, M. J. L., Smith, A., and Zimmermann, H. U. 1981, *Space Sci. Rev.*, **30**, 513.
van der Klis, M. 1986*a*, in *Physics of Accretion onto Compact Objects* (*Lecture Notes in Physics*, **266**) (Heidelberg: Springer), p. 157.
———. 1986*b*, in *Proc. Variability in Galactic and Extragalactic X-Ray Sources*, ed. A. Treves, in press.
van der Klis, M., Jansen, F., van Paradijs, J., Lewin, W. H. G., Sztajno, M., and Trümper, J. 1987*a*, *Ap. J.* (*Letters*), **313**, L19.
van der Klis, M., Jansen, F., van Paradijs, J., Lewin, W. H. G., van den Heuvel, E. P. J., Trümper, J., and Sztajno, M. 1985, *Nature*, **316**, 225.
van der Klis, M., Stella, L. White, N., Jansen, F., and Parmar, A. N. 1987*b*, *Ap. J.*, **316**, 411.

G. HASINGER and A. LANGMEIER: Max-Planck Institut für extraterrestrische Physik, 8046 Garching bei München, Federal Republic of Germany

W. H. G. LEWIN: Massachussetts Institute of Technology, Center for Space Research and Department of Physics, Room 37-627, Cambridge, MA 02139

L. STELLA and M. VAN DER KLIS: EXOSAT Observatory, ESTEC SAE, Postbus 299, 2200 AG Noordwijk, The Netherlands

J. VAN PARADIJS: Astronomical Institute "Anton Pannekoek," Roetersstraat 15, 1018 WB Amsterdam, The Netherlands